Light emission from spectral analysis of Au/MoS_2 nanocontacts stimulated by scanning tunneling microscopy

A. Carladous, R. Coratger,* F. Ajustron, G. Seine, R. Péchou, and J. Beauvillain
CEMES/CNRS, 29, rue Jeanne Marvig, Boîte Postale 4347, 31055 Toulouse, France
(Received 6 February 2001; revised manuscript received 27 December 2001; published 28 June 2002)

Due to a Volmer-Weber growth mode, the deposition of ultrathin gold films on molybdenite substrates leads to the formation of three-dimensional gold islands. The light emission detected on these islands has been attributed to a radiative decay of localized plasmons excited by inelastic tunneling electrons. This emission exhibits puzzling properties compared to what is usually observed on thicker gold films. Spectral analysis of emitted light enables current-voltage characteristics of the Au/MoS_2 interface to be determined at a nanometer scale.

DOI: 10.1103/PhysRevB.66.045401 PACS number(s): 78.20.Jq, 07.79.Cz

INTRODUCTION

The scanning tunneling microscope (STM) designed by Binnig and Rohrer[1] in 1981 allows conductive and semiconductive surfaces to be observed with a subnanometer resolution. Various applications of the STM have been made using different surface processes. Among these, photon emission in the tunnel junction of the microscope is particularly interesting when it comes to investigating surface properties at an atomic scale.

Photons have been detected on noble metals in ultrahigh vacuum[2] and in air.[3] This emission has been attributed to a radiative decay of a localized plasmon excited by inelastic tunneling electrons. In air, spectral analysis of the emitted light for Au-Au tunneling junctions has been performed.[4,5] Spectra studied as a function of tunneling current and surface bias voltage have shown similar, reproducible characteristics.

In this paper, an original application of light emission stimulated by STM is reported. Three-dimensional (3D) gold islands have been obtained by depositing very thin gold films on molybdenite substrates. Light emission has been detected on these islands and exhibits puzzling properties. Spectral analysis of the emitted light has been conducted on various islands. Following a comparison with the spectra usually obtained on thicker gold films, electrical properties of the Au/MoS_2 interface have been investigated.

EXPERIMENTAL SETUP

The experimental setup has already been described elsewhere.[6] A customized (pocket-size) STM operating in the constant current mode was adapted for photon detection. Optical fibres (core diameter$=1$ mm) placed at about 1 mm from the tunneling junction conveyed the emitted photons to a photomultiplier (PM) and a spectrometer. The PM (Hamamatsu R943-02) operates in the photon counting mode with a dark count rate of 20 count/sec at 255 K in the 185–900 nm range. The complete range has been used to draw up photon mappings of the scanned areas. The spectrometer consists of an optical multichannel analyzer (EG&G, OMA 1245) connected to a charge-coupled device detector cooled at 173 K and operating in the 300–1050 nm range. This experimental setup allows simultaneous acquisition of STM topography, related photon mapping and emission spectrum that represents the emitted photon number versus wavelength.

Tips were prepared by cutting 0.25-mm-diameter gold wires. Single molybdenite crystals provided by Wards Geology were used as substrates. Fresh surfaces were prepared by cleaving in air, producing atomically flat areas several μm^2 in size. After cleavage, the MoS_2 substrate ($6\times4\times1$ mm^3) was inserted into the evaporator and baked for 2 h at 350 °C. Gold was then evaporated on part of the substrate (4×4 mm^2) from a resistively heated molybdenum boat in 10^{-8} Torr vacuum with a deposition rate of about 2–5 Å s^{-1} to obtain a mean coverage thickness varying between 2 and 8 nm. Deposition rate was measured with a quartz-crystal oscillator. The substrate temperature was maintained during film deposition. Post-deposition annealing was then conducted at the same temperature for 15 min. Ohmic contact was obtained by means of a conductive silver cement on the bare part of the molybdenite substrate (2×4 mm^2).

As already shown using transmission electron microscopy[7,8] this experimental process results in epitaxial thin gold films growing under a Volmer-Weber mode: 3D particles or atom clusters first nucleate and then grow and coalesce with each other to form a continuous film depending on the deposited thickness.

RESULTS

Gold thickness: 8 nm

The island-by-island growth mode clearly appears on the tunneling topography shown in Fig. 1(a) ($V_s=2.1$ V, $I_t=5$ nA; area 400×400 nm^2). Islands of various shapes and surfaces can clearly be seen: two of them, hexagonal in shape, are denoted *A*. An island, denoted *B*, appears in the bottom right corner of the image. Another, denoted *C*, which has a surface of about 52 000 nm^2 can be observed in the middle of the topography.

On this sample, photon maps exhibit large contrasts that are functions of the tunneling current as clearly shown in Figs. 1(b) and 1(c). Figure 1(b) has been obtained at a bias voltage of 2.1 V and a tunneling current of 5 nA. The average light intensity depends on the islands. When the tip scans

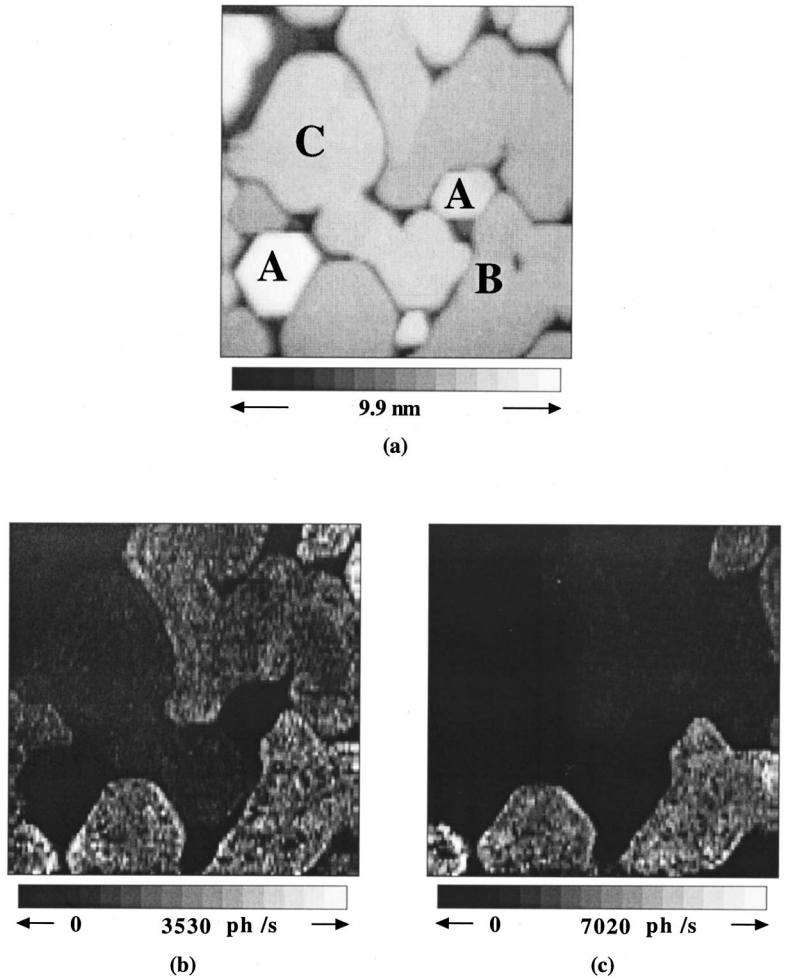

FIG. 1. (a) STM topography of a 8-nm-thick gold layer deposited on MoS_2 ($V_s = 2.1$ V, $I_t = 5$ nA). Three types of island are denoted *A*, *B*, and *C* respectively. (b) Simultaneous photon map of the same area ($V_s = 2.1$ V, $I_t = 5$ nA). (c) Photon map of the same area at $V_S = 2.1$ V and $I_t = 15$ nA.

hexagonal-shaped island (denoted *A*), only the dark count rate of the PM is observed. On the other hand, on island *B*, the average photon number is about 1800 photons/s versus 770 photons only on island *C*. Figure 1(c) shows a photon map acquired on the same area at the same bias voltage but with a tunneling current of 15 nA. Evolution of photon number with tunneling current differs according to the island considered. While the average light intensity is increasing with the tunneling current on island *B* (2560 photons/s are detected), a strong decrease in photon number appears on island *C* (only the dark count rate is measured). On hexagonal-shaped islands, emission yield remains insignificant.

This decrease in photon emission when tunneling current is increased has never been reported on thicker gold films. On the other hand, it has been clearly demonstrated using spectral analysis that light intensity always increases with tunneling current on a 100-nm-thick gold film.[4] To comprehend the different behaviors observed on these islands, particularly on the *C* type, emission spectra have been studied on various islands and compared to those previously obtained on thicker gold films.

Figure 2(a) shows four spectra acquired at two different bias voltages, **1.9 V** [spectra (*a*) and (*c*)] and **2.1 V** [(*b*) and (*d*)] on islands **B** [spectra (*c*) and (*d*)] and **C** [spectra (*a*) and (*b*)] of Fig. 1(a). Tunnelling current is set at 5 nA for an exposure time of 200 s. On island *B*, spectrum (*c*) presents two peaks at a bias voltage of 1.9 V centered at 1.44 and 1.72 eV. The experimental high-energy cutoff is measured at 1.92 eV and is in good agreement with the quantum law $E_{\max} = hc/\lambda_{\text{cutoff}} = eV_s$. It should be noted that this cutoff cannot be calculated from a power-law fit as in luminescence experiments on semiconductors because the experimental spectrum cannot be simply fitted by a mathematical function. Then, this value is estimated from the noise level of each spectrum with an accuracy of about 20 meV in this energy range. On island *C*, the emission spectrum (*a*) has not the same characteristics when bias voltage is maintained at 1.9 V. Indeed, a broad peak centred at 1.38 eV and a high-energy cutoff at 1.55 eV can clearly be seen on the emission spectrum (*a*).

When bias voltage increases, the same behavior is observed. On island *B*, the spectrum at 2.1 V presents two peaks at 1.44 and 1.77 eV and its high-energy cutoff is in good agreement with the quantum law. On island *C*, two peaks are also present but centred on different wavelengths: 1.44 and 1.59 eV. In this case, the high-energy cutoff (about 1.77 eV), is lower than the one computed.

On thicker gold films, peak position strongly depends on the tip used, while the high-energy cutoff is independent. This is demonstrated in Fig. 2(b). This emission spectrum

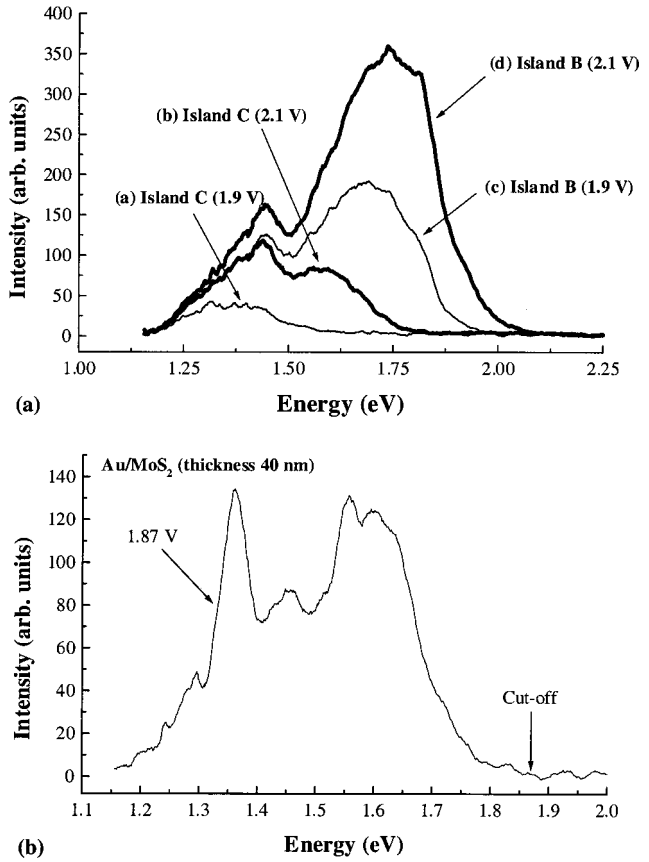

FIG. 2. (a) Spectroscopy of the emitted light carried out on islands *B* and *C* as shown in Fig. 1 at two different bias voltages: 1.9 and 2.1 V with the same tunneling current 5 nA. (b) Spectroscopy of light emitted from a continuous gold layer 40 nm in thickness deposited on MoS_2. The bias voltage is 1.87 V with a tunneling current of 5 nA. The arrow shows the cutoff energy given by the quantum law. A good agreement with the experimental threshold can be observed.

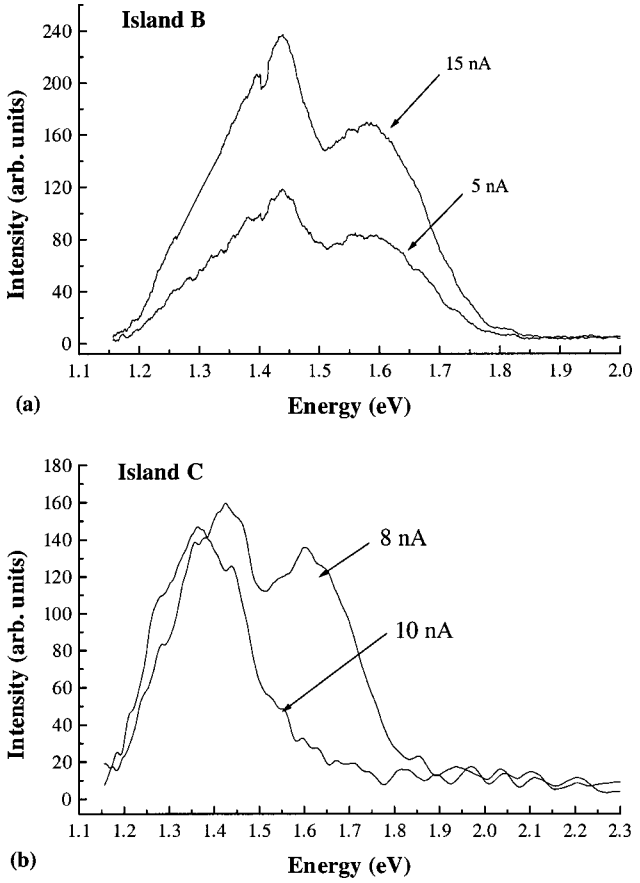

FIG. 3. (a) Spectroscopy on island *B* at 5 and 15 nA. Bias voltage is 1.7 V. (b) Same experiment on island *C* at 8 and 10 nA ($V_s = 2.3$ V).

has been obtained using another gold tip on a thick gold layer, 40 nm in thickness, deposited on the same MoS_2 substrate. In this case, the theoretical high-energy cutoff (indicated by an arrow) is in perfect agreement with the experimental one, while the peak number and peak wavelength are different from Fig. 2(a). Previous investigations on thick gold films deposited on glass and on mica have also demonstrated that this high-energy cutoff only depends on the bias voltage and follows the quantum law except for low bias voltages where a small offset of about 100 meV can be noted between the maximum energy of emitted photons and the maximum energy of injected electrons.[4,5] Other papers concerning STM induced photon emission spectroscopy in air on granular gold surfaces[9] and in UHV on thick layers of different metals also present the same characteristics for the cutoff wavelength.[10,11] Finally, recent papers concerning small metallic particles[12,13] show that the peak position in the spectra depends on the particle but the high-energy cutoffs are always constant.[13]

By comparison with these previous results concerning high-energy cutoffs, the spectra obtained on island *C* suggest that a voltage drop occurs on this island while island *B* behaves as a thin gold layer. The real voltage between the tip and the *C* island (V_{tun}) is not the one applied between the tip and the molybdenite substrate (V_s). Then, a voltage drop, $\Delta V = V_s - V_{\text{tun}}$, occurs at the metal/semiconductor interface. It can easily be calculated using the high-energy cutoff. For example, spectrum (*a*) acquired at $V_s = 1.9$ V on island *C* is typical of a spectrum that might be obtained at a real voltage of $V_{\text{tun}} = 1.5$ V applied between the tip and the gold island. Then, the Au/MoS_2 interface exhibits a voltage drop of 0.4 V. The same drop appears when bias voltage V_s increases to 2.1 V and spectrum (*b*) might be obtained at $V_{\text{tun}} = 1.7$ V on thicker gold layers. It should be noted that the same method has previously been used by Uehara *et al.* to obtain the voltage drop between small gold particles and an aluminum substrate through a thin oxide layer.[14] On the other hand, it should be pointed out that no voltage drop is measured on island *B*. Then, for this island, V_s is equal to V_{tun}.

The island behavior has also been studied in terms of tunneling current. Figure 3 shows the spectrum evolution as a function of I_t on *B* [Fig. 3(a)] and *C* [Fig. 3(b)] islands. Experiments were carried out with a constant exposure of 200 s. On island *B*, while bias voltage is set at 1.7 V, tunneling current is increased from 5 to 15 nA. Peak position (1.44 and 1.59 eV) and high-energy cutoff (at about 1.77 eV) are independent of the current. Then, on island *B*, emission yield

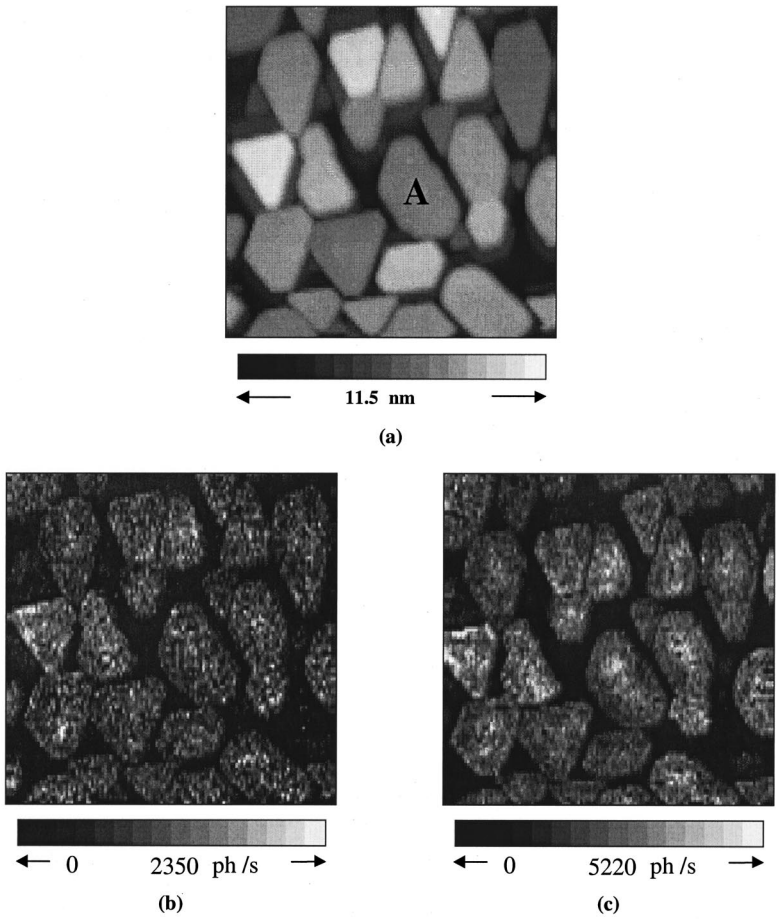

FIG. 4. (a) STM topography of a gold layer 5 nm in thickness deposited on MoS_2 ($V_s = 2.3$ V, $I_t = 2$ nA). (b) Simultaneous photon map of the same area ($V_s = 2.3$ V, $I_t = 2$ nA). (c) Photon map of the same area but at a tunneling current of 10 nA ($V_s = 2.3$ V).

is just enhanced when tunneling current is increased as is usually the case on thick gold films.[4]

On island *C*, the spectrum evolves very differently with tunneling current. Figure 3(b) presents two spectra at a constant bias voltage of 2.3 V with a tunnelling current of 8 and 10 nA (exposure time 200 s). It clearly appears that when the tunneling current is increased, light intensity decreases and the high-energy cutoff shifts to high values (estimated to be about 200 meV). The small shift observed in this case is due to the small increase of the tunneling current (from 8 to 10 nA). Larger shifts can be observed, for example, by doubling the current value. Moreover, while spectrum (*a*) presents two peaks centred at 1.44 and 1.59 eV, only one is present at 1.38 eV on spectrum (*b*).

Then, at 8 nA, this voltage drop at the Au/MoS_2 interface is 2.3-1.7=0.6 V [Fig. 3(a)]. The same method using the spectrum at 10 nA [Fig. 3(b)] gives $\Delta V = 0.8$ V (in good agreement with the shift of 200 meV observed between the two spectra in Fig. 3(b)). It has to be pointed out that this voltage drop is therefore increasing with the tunneling current. This has been observed on various islands on the 8-nm-thick film. This voltage drop also explains that no emission can be detected on some islands. For large ΔV values, the real voltage applied between the tip and the gold island is not high enough to allow a significant emission rate. The overall shape of the spectra is also strongly dependent on ΔV because the high-energy modes cannot be excited by tunneling electrons. On these particular islands, the spectra then present only one peak or a broad shoulder at high wavelength [see Fig. 2(a)]. To find a spectrum shape similar to the one obtained on a conventional island, it is necessary either to increase the bias voltage or to decrease the tunneling current. However, thinner films exhibit another behavior.

Gold thickness: 5 nm

Figure 4(a) presents the tunneling topography of a gold film, 5 nm in thickness, deposited on the MoS_2 substrate ($V_s = 2.3$ V, $I_t = 2$ nA). Surface consists in 3D islands with areas less than 10 000 nm^2 and a height of about 5 nm. This film exhibits equilateral-triangle-shaped and hexagonal-shaped islands, demonstrating that the Volmer-Weber growth mode occurs along the [111] direction. An island in the middle of the image is denoted *A*.

On this surface, photons are detected for a bias voltage higher than 2.1 V. Figure 4(b) shows the photon map acquired for a tunneling current of 2 nA and a bias voltage of 2.3 V. Emission rate is constant from one island to another. For example, the average photon number recorded on island denoted *A* is about 640 photons/s. When the tunneling current is increased, the overall photon yield increases in the same way throughout the island as shown in the Fig. 4(c), where tunneling current is set at 10 nA. In this case, 2240 photons/s are detected on island *A*.

Spectral analysis of emitted light has been performed on island *A* to assess the difference that can be noted on the

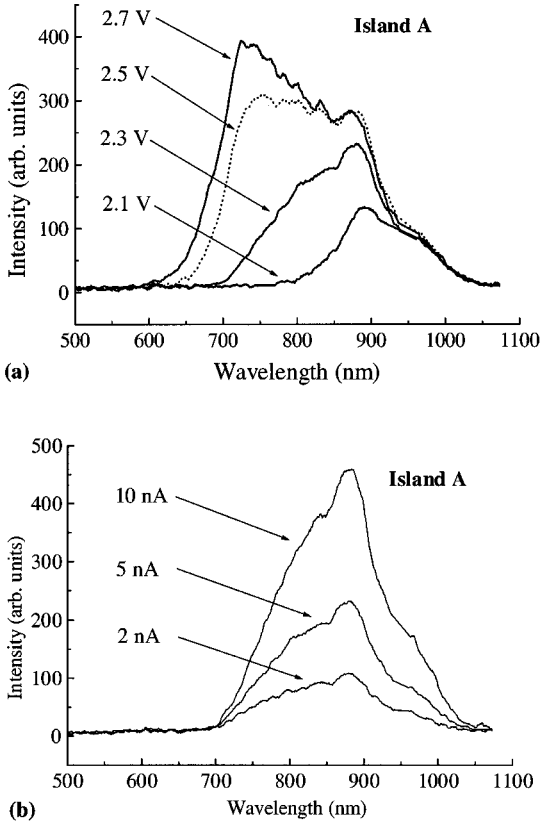

FIG. 5. Emission spectra of a 5-nm-thick gold layer deposited on MoS_2. (a) Experiments have been carried out on island *A* at four different bias voltages 2.1, 2.3, 2.5, and 2.7 V with a constant tunneling current ($I_t = 5$ nA). (b) Spectrum evolution in terms of tunneling current on the same sample ($V_s = 2.3$ V).

5-nm-thick gold layer relative to the 8-nm-thickness deposit. Figure 5(a) presents the spectrum evolution in terms of bias voltage in the 2.1–2.7 V range. In this case, the overall emission rate increases with applied bias voltage whereas a light intensity decrease is observed when bias voltage exceeds 2.7 V. New high-energy components are visible when V_s increases from 2.1 to 2.7 V (see the peak at 1.65 eV) and a blueshift in spectrum high-energy cutoff is also observed. The same spectrum evolution with bias voltages from 1.65 to 2.05 V has previously been observed on thicker gold films.[4,5] Using high-energy cutoffs, a constant voltage drop of 0.6 V can be measured at the Au/MoS_2 interface on island *A*. Then, a spectrum obtained on island *A* at 2.1 V corresponds to the one acquired at a voltage of 1.5 V that really exists between the tip and the gold island. At a fixed tunneling current, the voltage drop remains unchanged when bias voltage increases.

The evolution of this voltage drop as a function of tunneling current is shown in Fig. 5(b). These experiments have been conducted with I_t ranging from 2 to 10 nA for a bias voltage set at 2.3 V. An increase in emission yield is clearly shown but emission wavelengths do not change when the tunneling current varies: a peak centred at 1.4 eV clearly appears on the different spectra. Moreover, high-energy cutoffs of spectra remain unchanged and can be observed at 1.75 eV. On thick gold layers, such thresholds are observed

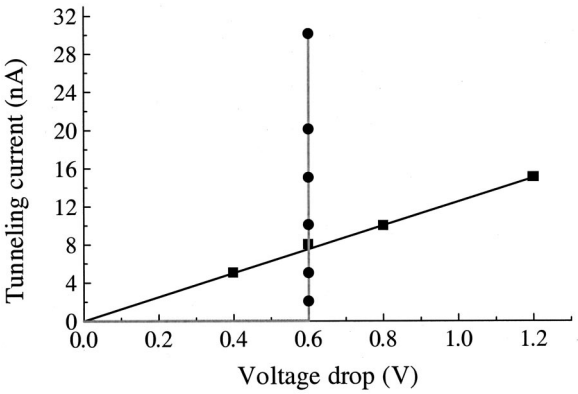

FIG. 6. Current-voltage characteristics of the Au/MoS_2 interface obtained on both samples: 8-nm-thick gold sample (small square) and 5-nm thick gold sample (small circle).

at a bias voltage of 1.7 V.[5] Then, it can be concluded that the real voltage between the tip and gold island is 1.70 V and a voltage drop of 0.6 V appears at the metal/semiconductor interface. Moreover, this voltage drop is independent of the tunneling current.

DISCUSSION

The metal/semiconductor interface can be electrically characterized by spectral analysis of the emitted light. Indeed, current-voltage characteristics at the interface are obtained using the voltage drop variations with tunneling current. Figure 6 represents this evolution for films of different thicknesses: data symbolized by a square have been obtained on the 8-nm-thick film on island *C* (Fig. 1), whereas those represented by a circle have been acquired on 5-nm-thick gold film on island *A* (Fig. 4). These current-voltage characteristics differ greatly from one film to another: while voltage drop is proportional to the tunneling current for the 8-nm-thick film, it remains unchanged in terms of tunneling current on 5-nm-thick gold films. Therefore, it can be concluded that there exists a resistance at the metal/semiconductor interface for the 8-nm-thick layer and its calculated value is 80 Mohms. On the 5-nm thick layer, the interface behaves as a

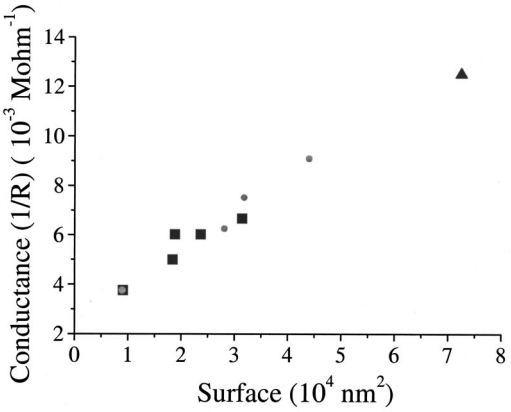

FIG. 7. Conductance variations in terms of island surface deduced from photon spectroscopy measurements.

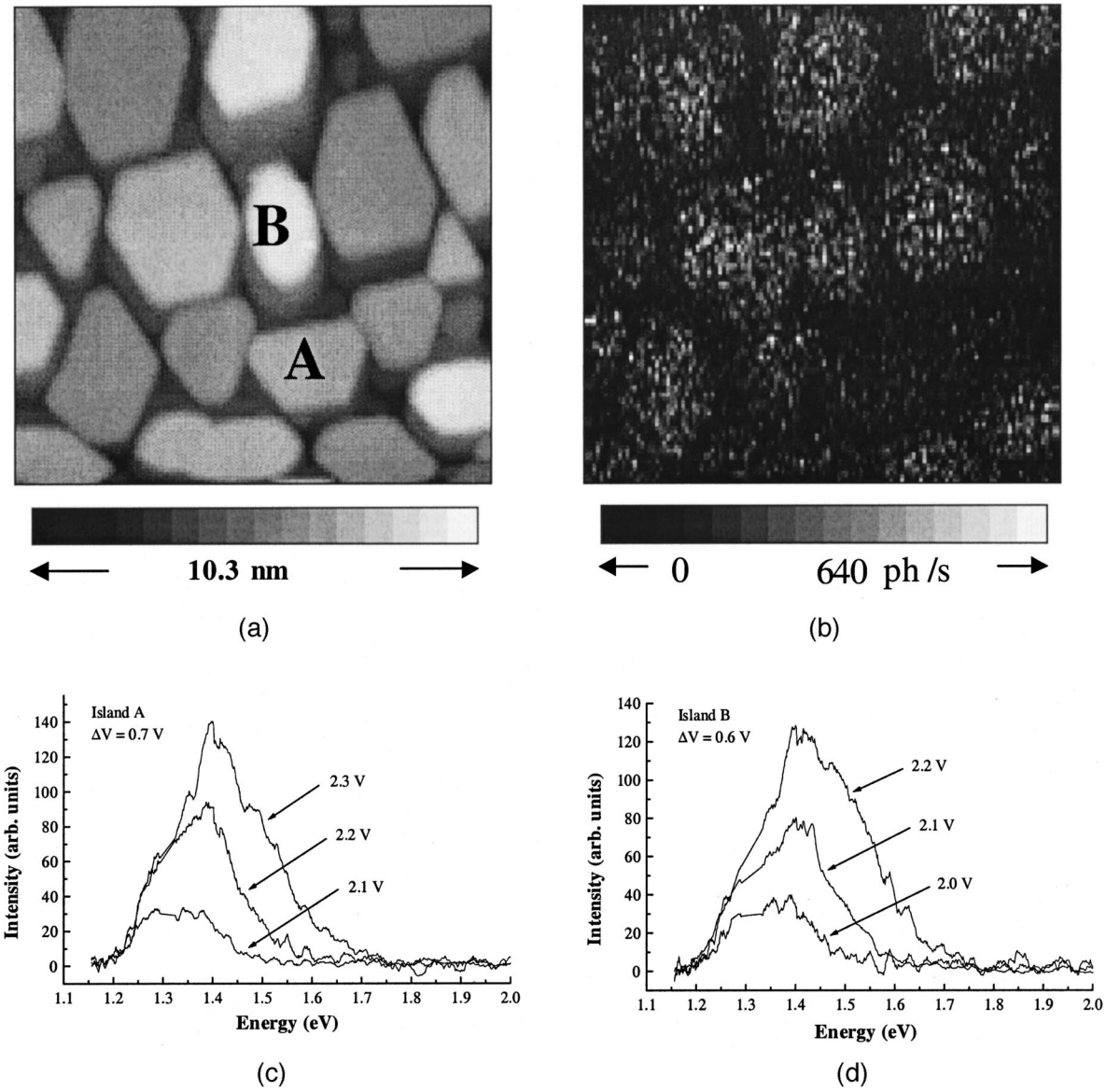

FIG. 8. (a) STM topography of a 5-nm-thick gold layer deposited on MoS_2 ($I_t = 2$ nA). (b) Simultaneous photon map. Two island noted *A* and *B* in the topography give different emission yields. (c) Emission spectra performed on island *A* at three different bias voltages. From the high-energy cutoffs, a voltage drop of 0.7 V has been obtained ($I_t = 15$ nA). (d) Same experiments carried out on island *B*. In this case, the measured voltage drop is 0.6 V ($I_t = 15$ nA).

Schottky junction with a threshold voltage of 0.6 V. This is confirmed by the fact that tunneling is impossible for bias voltages below this value. The measured threshold voltage can be compared to the Schottky barrier height of the Au/MoS_2 contact given by Mönch[15] and is equal to 0.8 V. The threshold voltage is logically found to be lower than the Schottky barrier height.[16]

The presence of an interface resistance has been demonstrated on the 8-nm-thick film for island *C* (Fig. 1). As different emission yields have been observed on various islands for the same tunneling conditions [Fig. 1(b)], one can measure the resistance of the metal/semiconductor interface for each island. It appears that the resistance value is strongly dependent on island area. Figure 7 shows the evolution of the interface conductance with island area. While the data symbolized by a square and a circle have been obtained from two different gold tips on the same 8-nm-thick film, the result represented by a triangle has been acquired on another 8-nm-thick gold deposit. The measured conductance is proportional to the island surface whatever the tip and provided the gold thickness is 8 nm. Its value is typically 4×10^{-3} $Mohm^{-1}$ per 10^4 nm^2 and typical resistance values are in the 100 Mohms range. This surface-dependent resistance also accounts for the fact that each island yields a characteristic emission rate.

The second study performed on 5-nm-thick layers demonstrates that the junction behaves as a Schottky contact and then, each nanojunction can be studied separately. On a few photon maps, the emission rate is found to depend on the observed islands. An example is given in Fig. 8. Tunneling

topography [Fig. 8(a)] and photon map [Fig. 8(b)] have been acquired at 2.1 V and 2 nA. Two islands, one hexagonal in shape and another ellipsoidal are denoted *A* and *B*, respectively. On a photon map, a contrast between these two islands can be observed: 300 photons/s are recorded on island *B*, whereas only the dark count rate of the photomultiplier is observed when the tip scans island *A*. The lack of photon emission on this island is due to the low tunneling current and the local voltage drop. To understand this difference in light intensity, the spectral analysis of emitted light has been performed on islands *A* and *B* using a higher tunneling current (15 nA). Due to the rectifying behavior of these nanocontacts, the voltage drop remains the same. Figures 8(c) and 8(d) present the spectrum evolution with bias voltage on islands *A* and *B*, respectively. Bias voltage varies between 2.1 and 2.3 V for the hexagonal-shaped island and between 2.0 and 2.2 V for island *B*. Spectrum acquired at 2.0 V on island *B* corresponds to the one obtained on island *A* at a bias voltage fixed at 2.1 V. Then, for the island *A*, a voltage drop of 0.7 V can be measured whereas a 0.6 V drop appears for island *B*. On each island, this drop is found to be independent of the tunneling current. Therefore, both islands exhibit a Schottky behavior and two different threshold voltages are observed. As the islands have similar areas, this difference can be explained by two different Schottky barrier heights at the metal/semiconductor interface. An effect of the island height has also to be rejected because Fig. 8(a) clearly demonstrates that a greater part of the islands surrounding *A* exhibits the same height but a constant voltage drop of 0.6 V. These observations cannot be accounted for by a different crystallographic orientation at the nanometer scale. The presence of localized defects on the molybdenite substrate surface below island *A* can therefore be put forward to explain the different Schottky barrier heights. Indeed, unlike suggestions by previous studies using transmission electron microscopy, Ichinokawa *et al.*[17] have shown by scanning tunnelling microscopy that very few defects exist on a molybdenite surface cleaved in air. That could explain why different barrier heights have seldom been observed in this study.

Spectroscopic imaging experiments on these thin gold layers have also been performed. Direct $I(V)$ plots are not usable because the voltage drop at the interface prevents from knowing exactly the bias voltage applied between the tip and the island. Then, spectroscopic imaging can be used to observe the peculiar behavior of each contact. Figure 9(a) shows a topography of the gold layer 8 nm in thickness at a bias voltage of 650 mV. The central part exhibits a triangular island surrounded by larger ones. Figure 9(b) has been obtained using a constant modulation of the bias voltage of 150 mV during the scan and representing the induced variations of the tunneling current shown in gray levels [$\Delta I(\Delta V)$ imaging]. This image clearly demonstrates that the small island behaves differently from the surrounding layer because the induced current variations are larger on this triangular structure. It should be noted that this effect disappears at high voltage (typically above 1 V). The voltage drop at the interface again explains this observation because it induces a slight decrease of the tip-sample distance when the tip scans the island. Then, the current variations are measured on a

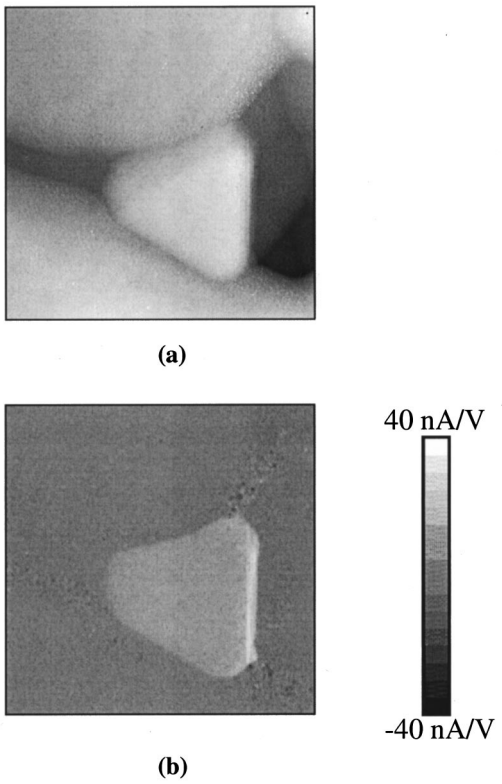

FIG. 9. (a) Topography of the 8-nm-thick gold layer ($120 \times 120\ \mathrm{nm}^2$) performed at a bias voltage of 0.650 mV. (b) $\Delta I(\Delta V)$ spectroscopic image of the same area. The bias voltage modulation is 0.150 mV. A significant contrast appears on the triangular gold island.

$I(V)$ curve calculated for a smaller tip-sample distance. At low voltage, the slope of the $I(V)$ curve increases as the distance decreases because, for a given distance, the voltage threshold at which the tunneling current flows in the STM junction is smaller when the tip is close to the sample. At high voltage, the $I(V)$ curves are almost parallel and the contrast disappears. However, it is impossible from these experiments to obtain the voltage drop at the interface or the electrical characteristics of the nanocontacts. Photon emission experiments remain the unique tool to perform such measurements.

The behavior of small Ag and Au particles has been already studied using photon emission experiments by Kinnon *et al.*[18] and Uehara *et al.*[14] In this last reference, small voltage drops of about 50 meV in the photon spectra of small Au particles deposited on oxidized Al surfaces have been presented.[14] The authors suggest that this effect is related to Coulomb blockade due to the small capacitance of the tip-particle and particle-substrate junctions. Then, they demonstrate that single-electron charging effects can be observed even at room temperature using photon emission spectroscopy. This interpretation could also be used in the case of Au islands on MoS_2. Further experiments using thinner gold films with very small gold islands are in hand to comprehend this intriguing behavior and particularly the large voltage drops that have been obtained. More generally, these results

also suggest that light emission can be used to study the electrical characteristics of nanoobjects without physical contact.

CONCLUSION

By conducting a spectral analysis of the light emitted in the STM junction, it has been demonstrated that current-voltage characteristics of Au/MoS_2 nanojunctions can be obtained. On 8-nm-thick deposits, an interface resistance has been observed. It has equally been shown that the measured conductance is proportional to the island area and that resistance values are about 100 Mohms. On 5-nm-thick deposits, each island exhibits a Schottky junction behavior at the interface. Different barrier heights have been observed and molybdenite surface defects are invoked to account for these observations.

Further studies are planned to comprehend the different findings on both thicknesses and to explain the transition between the contact resistance and the Schottky junction. Besides, in the case of a Schottky behavior it will be interesting to study the influence of surface defects on the threshold voltage value and then, the evolution of the Schottky barrier height. Indeed, defects can easily be created by Ar^+ ion bombardment as already performed by Lince, Carré, and Fleischauer.[19] The study of these current-voltage characteristics at the nanometer scale can be also extended to other layered substrates such as WSe_2 and WS_2. Indeed, Rettenberger *et al.*[20] have shown that growth of gold on these substrates also follows the Volmer-Weber mode.

ACKNOWLEDGMENT

The authors would like to thank S. Reyjal for her technical assistance.

*Corresponding author: Email address: coratger@cemes.fr

[1] G. Binning, H. Rohrer, Ch. Berger, and E. Weibel, Appl. Phys. Lett. **40**, 178 (1982).
[2] J. K. Gimzewski, B. Reihl, J. H. Coombs, and R. R. Schlitter, Z. Phys. B: Condens. Matter **72**, 497 (1988).
[3] V. Sivel, R. Coratger, F. Ajustron, and J. Beauvillain, Phys. Rev. B **45**, 8634 (1992).
[4] R. Péchou, R. Coratger, C. Girardin, F. Ajustron, and J. Beauvillain, J. Phys. III **6**, 1441 (1996).
[5] R. Péchou, R. Coratger, F. Ajustron, and J. Beauvillain, Appl. Phys. Lett. **72**, 671 (1998).
[6] R. Coratger, Thèse de l'Université Paul Sabatier, Toulouse, 1991.
[7] T. P. Darby and C. M. Wayman, Phys. Status Solidi A **25**, 585 (1974).
[8] G. Honjo, K. Takayanagi, K. Kobayashi, and K. Yagi, Phys. Status Solidi A **55**, 353 (1979).
[9] M. M. J. Bischoff, M. C. M. M. van der Wielen, and H. van Kempen, Surf. Sci. **400**, 127 (1998).
[10] R. Berndt, Ph.D. Thesis, Basel, 1992.
[11] J. H. Coombs, J. K. Gimzewski, B. Reihl, J. K. Sass, and R. R. Schlittler, J. Microsc. **152**, 325 (1988).
[12] F. Silly, A. O. Gusev, A. Taleb, F. Charra, and M. P. Pileni, Phys. Rev. Lett. **84**, 5840 (2000).
[13] N. Nilius, N. Ernst, and H. J. Freund, Phys. Rev. Lett. **84**, 3994 (2000); Surf. Sci. **478**, L327 (2001).
[14] Y. Uehara, S. Ohyama, K. Ito, and S. Ushioda, Jpn. J. Appl. Phys., Part 2 **35**, L167 (1996).
[15] W. Mönch, Appl. Phys. Lett. **72**, 1899 (1998).
[16] H. Mathieu, *Physique des Semiconducteurs et des Composants Électroniques* (Editions Masson, Paris, 1990), p. 244.
[17] T. Ichinokawa, T. Ichinose, M. Tohyama, and H. Itoh, J. Vac. Sci. Technol. A **8**, 500 (1989).
[18] A. W. McKinnon, M. E. Welland, T. M. H. Wong, and J. K. Gimzewski, Phys. Rev. B **48**, 15 250 (1993).
[19] J. R. Lince, D. J. Carré, and P. D. Fleischauer, Phys. Rev. B **36**, 1647 (1987).
[20] A. Rettenberger, P. Bruker, M. Metzler, F. Mugele, Th. W. Matthes, M. Böhmisch, J. Boneberg, K. Friemelt, and P. Leiderer, Surf. Sci. **402–404**, 409 (1998).